Studying parameters of turbulent wakes for model wind turbines

Cite as: AIP Conference Proceedings **2027**, 030086 (2018); https://doi.org/10.1063/1.5065180
Published Online: 02 November 2018

S. V. Strijhak, K. B. Koshelev, and A. S. Kryuchkova

Studying Parameters of Turbulent Wakes for Model Wind Turbines

S. V. Strijhak[a)], K. B. Koshelev[b)], and A. S. Kryuchkova[c)]

Ivannikov Institute for System Programming of the Russian Academy of Sciences
109004, Moscow, Russia

[a)]Corresponding author:strijhak@yandex.ru
[b)]koshelevkb@mail.ru
[c)]pudjic@gmail.com

Abstract. The wind energy is an important part of renewable energy. The wind farms can operate in various climatic conditions on a large territory of Russian Federation. The features of numerical simulation of turbulent flows using the OpenFOAM package and SOWFA library are considered. The mathematical model has the equations for mass, momentum and energy conservation for incompressible flow. Large-eddy simulation has been applied in the context of wind turbines operation. Lagrangian-averaged scale-independent dynamic Smagorinsky model is used. Two solvers ABLSolver and pisoFoamTurbine have been used for simulations. The results of computations for two test cases (2 and 12 wind turbines) with definition of the main flow parameters are given, the efficiency of the applied solver is shown.

INTRODUCTION

The wind energy is an important part of renewable energy sources. The development of wind energy industry in Russian Federation involves designing and operation of new wind power plants and turbines. The wind farms can operate in various climatic conditions on the large territory of the country (Ulyanovsk region, Republic of Adygea, Taman Peninsula, Arctic region). These processes raise a number of fundamental scientific and applied problems.

The scientific community are now studying the dynamics of turbulent wakes for wind turbines and their performance [1]. Large-eddy simulation (LES) has recently been well applied in the context of wind turbines over flat and complex terrains [2]. An open-source library SOWFA (Simulator for On/Offshore Wind Farm Application) as part of OpenFOAM, which includes several incompressible solvers and utilities, was developed in NREL, Colorado, USA and is used by research community [3].

The mathematical model in SOWFA has the equations for mass, momentum and energy conservation for incompressible flow. The large-scale vortex structures can be simulated by means of integration the filtered equations. The box filter is used for receiving the filtered equations. The small eddies, for which the size don't exceed a size of grid cell, are modelled by means of different dynamic Smagorinsky models. The mathematical method is based on finite-volume method with second order accuracy. The values are defined in the centers of cells. The equations for coupling of velocity, pressure can be solved by means of iterative algorithm PISO, PIMPLE algorithms [4]. One of the solver ABLSolver can be used for Atmospheric Boundary Layer (ABL) simulation, another one - pisoFoamTurbine solver, which uses Actuator Lines Model, represents the work of wind turbine. The wind turbine may be defined as a number of profiles with a tabulated aerodynamics data. LES solves the filtered Navier-Stokes equations in which body forces from the turbine model are imposed. The calculation is carried out using standard and Lagrangian dynamic Smagorinsky's model for definition of subgrid scale turbulent viscosity [5, 6].

International Conference on the Methods of Aerophysical Research (ICMAR 2018)
AIP Conf. Proc. 2027, 030086-1–030086-8; https://doi.org/10.1063/1.5065180
Published by AIP Publishing. 978-0-7354-1747-2/$30.00

DESCRIPTION OF THE EXPERIMENTAL SETUP

We considered the first test case Blind Test 4 with 2 model wind turbines in wind tunnel of the Norwegian University of Science and Technology (NTNU) in Trondheim (Fig. 1).

These experiments were carried out to obtain the data base for verification of different numerical methods specializing on wind turbine modeling. The operational modes of one and two prototyping wind turbines, the optimum distance between aligned two turbines and the initial conditions effect on the total generated power were studied. The closed rectangular working section of wind tunnel had the width of 2.71 m, the height of 1.81 m and length of 11.15 m [7]. The tunnel had the ability to produce a uniform constant speed across the entire working area. Each of the prototyping turbines had 3 blades with variable cross section and variable twist angle and with the same airfoil NREL S826 from root to tip. The outer diameters of the upstream turbine T1 and the downstream turbine T2 were D1=0.944 m and D2=0.894 m respectively. The tower of T1 was cylindrical while the tower of T2 was constructed from four stepped cylindrical surfaces. The turbines were installed on the center line of the wind tunnel working area, the height of the rotors were adjusted in such a way that the axis of the two turbines were at the height of 0.827m from the bottom surface of the working area. The first turbine was placed at a distance of x=2D from the inlet cross section of the tunnel, where D=D2=0.894 m. The second turbine was placed at a distance of x/D = 5.18 from the first turbine [8]. A uniform inflow field with low turbulence intensity I=0.23% was studied in this work. The characteristic velocity was UREF=11.5 m/s and was equal to the velocity at the inlet. The velocity ratios λ for the first and the second turbines were equal to $\lambda T1=6$ and $\lambda T2=4.5$, respectively. Relatively low Reynolds numbers $Re \approx 10e5$ were observed near the turbines with such experimental conditions.

FIGURE 1. Schematic of integrated pre-burners/main

We also studied an example with 12 wind turbine in wind tunnel of EnFlo Laboratory in University of Surrey, UK [9]. This case was a test with 3-wide x 4-deep array (Fig. 2). The diameter of rotor was D = 416 mm. The velocity was set to Uref=1.5 m/s. Atmospheric Boundary Layer model was introduced to represent experimental conditions. The parameters of Neutral ABL, used in our simulation, are listed in Table 1 of work [10]. Each of the prototyping turbines had 3 blades with constant cross section. The blade was made of carbon fibre with a shape of a twisted thin flat plate, 0.8 mm thick, without an aerofoil cross-section. The rotor was designed for and operated at a tip-speed ratio (TSR) = 6. Velocity measurements were made using a Dantec two-component 40 MHz frequency-shifted Laser Doppler anemometry system. The wake profiles in a neutral, stable, unstable boundary layer, mean velocity profiles, profiles of the streamwise Reynolds stress, profiles of mean temperature and vertical heat flux were collected and processed in experiments.

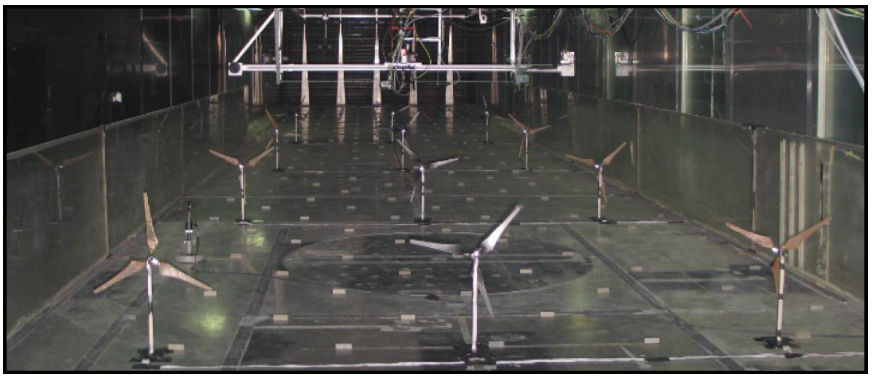

FIGURE 2. 12 wind turbines in wind tunnel

MATHEMATICAL FORMULATION AND PARAMETERS OF A NUMERICAL MODEL

The system of equations

In this work approach based on Large-Eddy Simulation (LES) with use of finite volume method for the solution of the main equations reflecting conservation laws was used for simulation parameters in Atmospheric Boundary Layer: the continuity Eq. (1), momentum Eq. (2), transport of scalar value - potential temperature Eq. (3). The subgrid-scale models are an important part of LES for ABL. The SGS stress tensor was arised from the filtering of the Navier-Stokes equations. Boussinesq approximation for buoyancy force is included through separate term in the momentum equation. The final mathematical model included the following Eq. (1)-(8).

$$\frac{\partial \bar{u}_j}{\partial x_j} = 0 \tag{1}$$

$$\frac{\partial \bar{u}_i}{\partial t} = -\frac{\partial}{\partial x_j}\left(\bar{u}_j \bar{u}_i\right) - \frac{\partial R_{ij}^D}{\partial x_j} - \frac{\partial \bar{p}}{\partial x_i} - \left(\frac{\partial \bar{p}}{\partial x_i}\right)^d + \left(1 - \frac{\bar{\theta}}{\bar{\theta}^0}\right) g_i + \epsilon_{ij} f^c \bar{u}_j \tag{2}$$

$$\frac{\partial \bar{\theta}}{\partial t} = -\frac{\partial}{\partial x_j}\left(\bar{u}_j \bar{\theta}\right) - \frac{\partial R_{\theta j}}{\partial x_j} \tag{3}$$

$$R_{ij}^D = -2\nu^{SGS}\bar{S}_{ij} \tag{4}$$

$$\bar{S}_{ij} = \frac{1}{2}\left(\frac{\partial \bar{u}_i}{\partial x_j} + \frac{\partial \bar{u}_j}{\partial x_i}\right) \tag{5}$$

$$\nu^{SGS} = (C_s\Delta)^2\left(2\bar{S}_{ij}\bar{S}_{ij}\right)^{1/2} \tag{6}$$

$$R_{\theta j} = -\frac{\nu^{SGS}}{Pr_t}\frac{\partial \bar{\theta}}{\partial x_j} \tag{7}$$

$$\frac{\partial R_{ij}^D}{\partial x_j} = -\frac{\partial}{\partial x_j}\left(\nu^{SGS}\frac{\partial \bar{u}_i}{\partial x_j}\right) - \frac{\partial}{\partial x_j}\left[\nu^{SGS}\left(\frac{\partial \bar{u}_j}{\partial x_i} - \frac{2}{3}\frac{\partial \bar{u}_k}{\partial x_k}\delta_{ij}\right)\right] \tag{8}$$

where, $\bar{u}_j$ is the resolved Cartesian velocity field, $R_{ij}^D = R_{ij} - Rkk\delta/3$ is the deviatoric part of the sub-grid-scale (SGS) stress tensor and R_{ij} is the SGS stress tensor. $\left(\frac{\partial \bar{p}}{\partial x_i}\right)^d$ is as partially constant driving pressure gradient term used to achieve a specified mean geostrophic wind, $\bar{\theta}$ is the resolved virtual potential temperature, $\bar{\theta}^0$ is the reference virtual potential temperature, g_i is the gravity vector, ϵ_{ij} - is the alternating symbol, f^c is the Coriolis parameter, and the subscripts 1, 2, and 3 refer to the x-, y-, and z-directions, respectively. $\bar{\theta}^0$ is set to the initial virtual potential temperature below the capping inversion of 300 K.

SOWFA allows to model wind turbines either with Actuator Lines or Actuator Disk models. The model in pisoFoamTurbine solver includes the continuity Eq. (1), momentum equation with additional force term (9):

$$\frac{\partial \bar{u}_i}{\partial t} = -\frac{\partial}{\partial x_j}\left(\bar{u}_j \bar{u}_i\right) - \frac{\partial R_{ij}^D}{\partial x_j} - \frac{\partial \bar{p}}{\partial x_i} + fi \tag{9}$$

where $\tilde{p}$- pressure, R_{ij}^{D} - so- called deviatoric part of the sub-grid-scale (SGS) stress tensor, fi - additional force term.

Considering the characteristic sizes of wind turbine blades, Re numbers can reach an order of Re=10e7-10e8. It is difficult to resolve all flow scales by means of LES since too big numerical grids would be required for this purpose. It is well-known that Actuator Line Model (ALM) approach doesn't demand too detailed grids around the turbine blades. This approach allows to represent various types of vortexes, wake, trailer, root and boundaries vortexes. In scope of ALM turbine blades are approximated by separate flat sections with given profile, chord and twist. Values of lift and drag forces are collected in tables for each profile. The force projected on the flow is equal to the aero dynamical force applied on operating turbine blades. Procedure of force projection comes to a number of separate terms adding in the momentum equation. The resultant force fi is determined with following technique:

$$f_i^{turbine}(r) = \frac{F_i^{actuator}}{eps^3 \pi^{\frac{3}{2}}} * \exp\left[\left(-\frac{r}{eps}\right)^2\right], \tag{10}$$

where $F_i^{actuator}$ is actuator point force, projected as a body force onto Computational Fluid Dynamics (CFD) grid, r - distance between CFD cell center and actuator point, eps is of Gaussian filter width related to the initial intermittency. Further details can be found in [11].

Boundary and Initial conditions

The simulation is run in 3D box domain. The numerical technique comprised a preliminary simulation with ABLSolver aimed to define the inlet parameters for the major domain with rotating wind turbines, the second step consisted in numerical simulations using pisoFoamTurbine. The value of numBladePoints for the case with 12 wind turbines was set to 40, the epsilon value was set to 5.0.

Numerical schemes and solvers

The Gauss linear Scheme was used for approximation of convective terms, the Gauss linear corrected scheme was used approximation of laplacian terms. To solve linear system equations the PBiCG method with DILU preconditioner was used for velocity, temperature and the GAMG method was used for pressure. The tolerance was set to 1e-6.

Computational domain and mesh

The computational domain constituted a parallelepiped with dimensions from (0 -1.355 0) to (11.15 1.355 1.8) meters in which there were 2 prototyping wind turbines. The wind turbines were located at the positions of (1.788 0.0 0.0) and (0.0 4.47 0.0) meters.

A hexahedral computational mesh was built using the standard blockMesh utility, then the area near the turbines including the wakes was selected and the mesh in this area was refined by the refineMesh utility [12]. An unstructured 4-million and 8 million meshes was used for the simulation. The mesh had a refinement within the wake area (Fig. 3). For the case with 12 wind turbines the refinement in the mesh was done for the tower and nacelle of each wind turbine (Fig. 4).

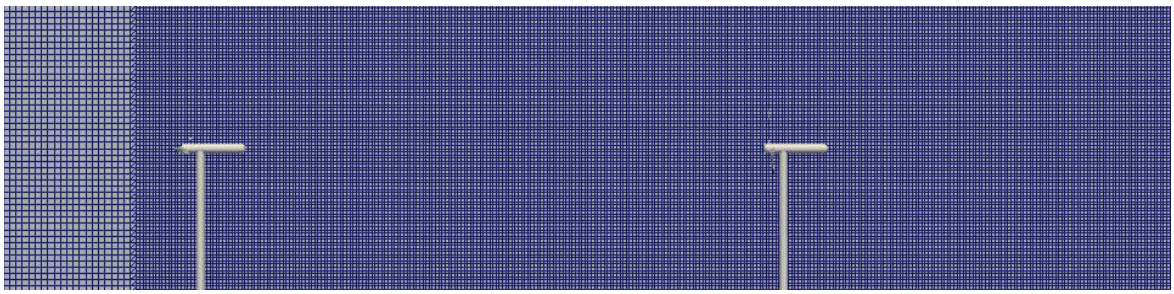

FIGURE 3. The computational domain and the mesh for Blind 4 test case

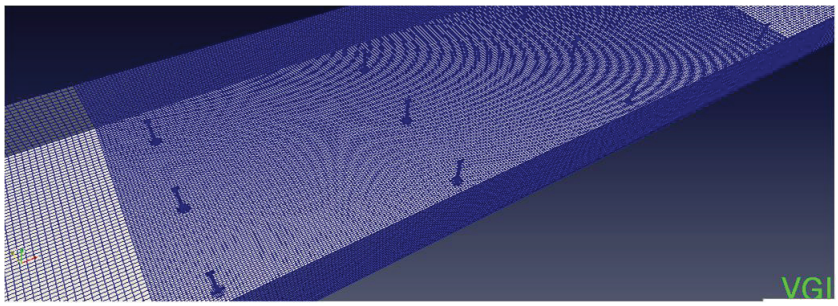

FIGURE 4. Fragment of the computational mesh

Process of computations

The computations were performed on the UniHUB cluster of the ISP RAS using 36-72 cores. The time step was set so that the maximum Courant number did not exceed 0.75. The time step was equal to 0.0005. The continuation of the computation with 2 seconds for 2 wind turbines and 20 seconds for 12 wind turbines did not reveal any changes in the spatial distribution of variables.

RESULTS OF COMPUTATIONS AND DISCUSSION

As a result of flow simulation in the wake for the three-bladed wind turbine the average and instantaneous values of velocity, pressure, subgrid kinetic energy, turbulent viscosity, components of stress tensor were calculated, the power and trust coefficients, the velocity normalized by Uref. The vorticity, velocity fields and normalized velocity are shown on Fig. 5–7. The results of velocity field prediction were improved by introducing the tower and the hub geometry to the model [12]. The final maximum discrepancy for the normalized velocity amounts to 8% that indicates a good accuracy for engineering calculations (Fig. 7).

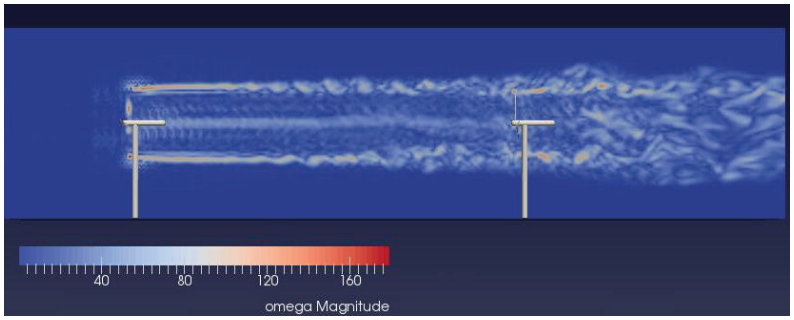

FIGURE 5. Vorticity field at t=2 s

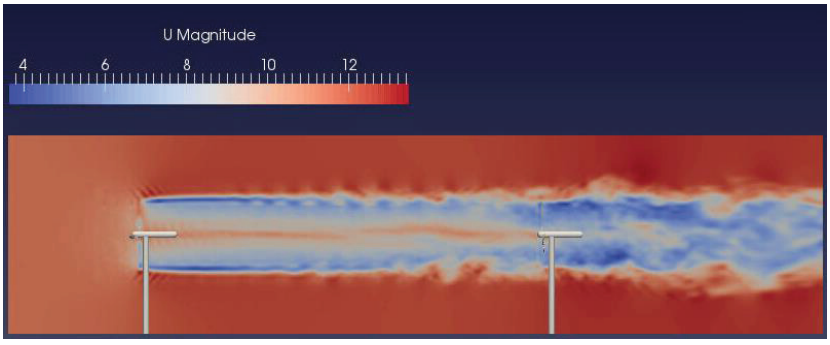

FIGURE 6. Velocity field at t=2 s

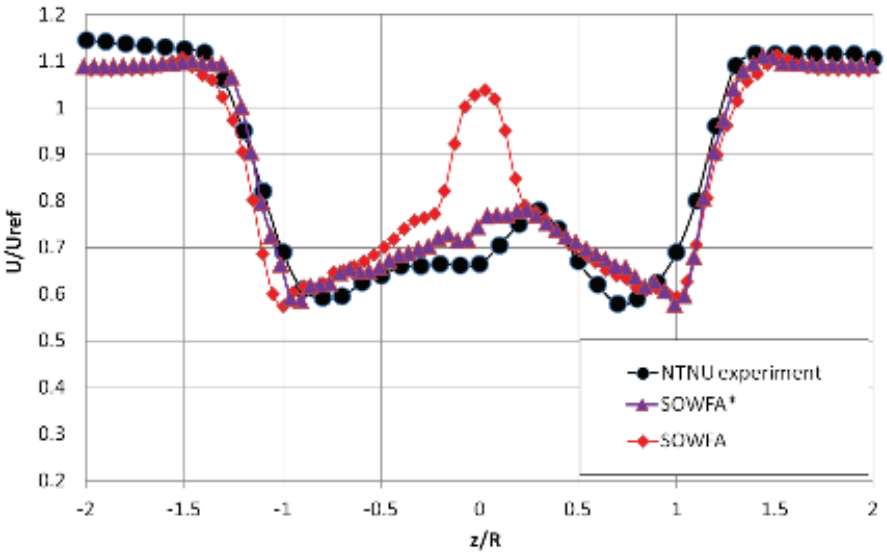

FIGURE 7. Profile of velocity normalized by Uref

The same investigation was done for case with 12 wind turbines. The solvers allow distinguishing the mean and turbulent wake flows behind turbines in series and the behavior of the whole 12-turbines array (Fig. 8). The flow patterns around four turbines aligned to the axis of symmetry of the array were studied to determine general behavior of the resulting flow in ABL. It was noted that the wakes behind the first turbines row are more stable, but with the second turbines row the wake turbulent behavior becomes more pronounced (Fig. 9).

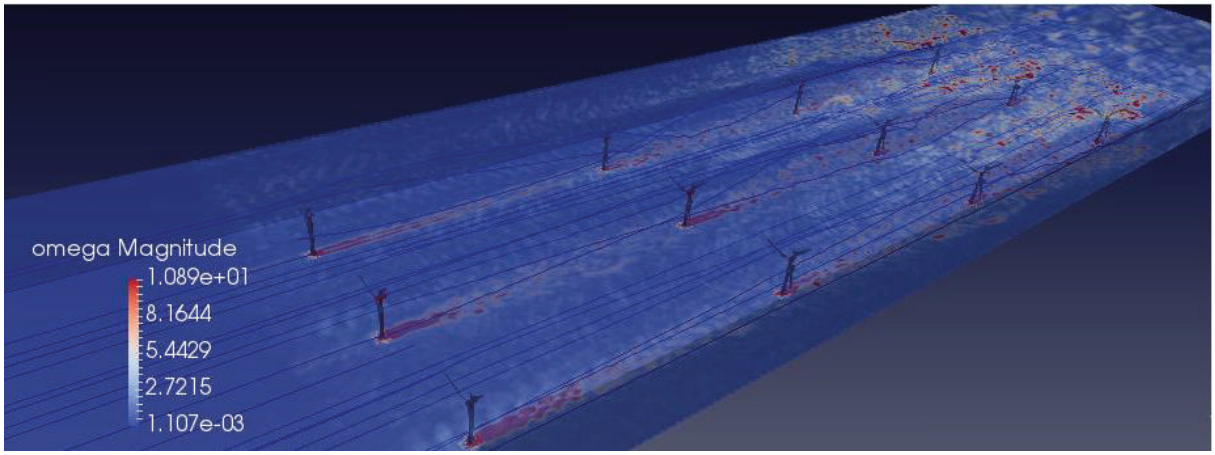

FIGURE 8. Structure of velocity (time = 20 seconds)

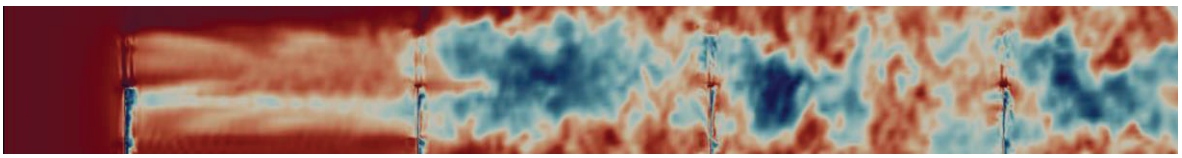

FIGURE 9. Turbulence behavior of the interaction between wind turbine and ABL

The results of calculation of the horizontal velocity profiles behind the wind turbines are shown in Fig. 101. The difference with experiment's values of velocity profiles in different sections can be explained by using ALM model to simulate flow around wind blades.

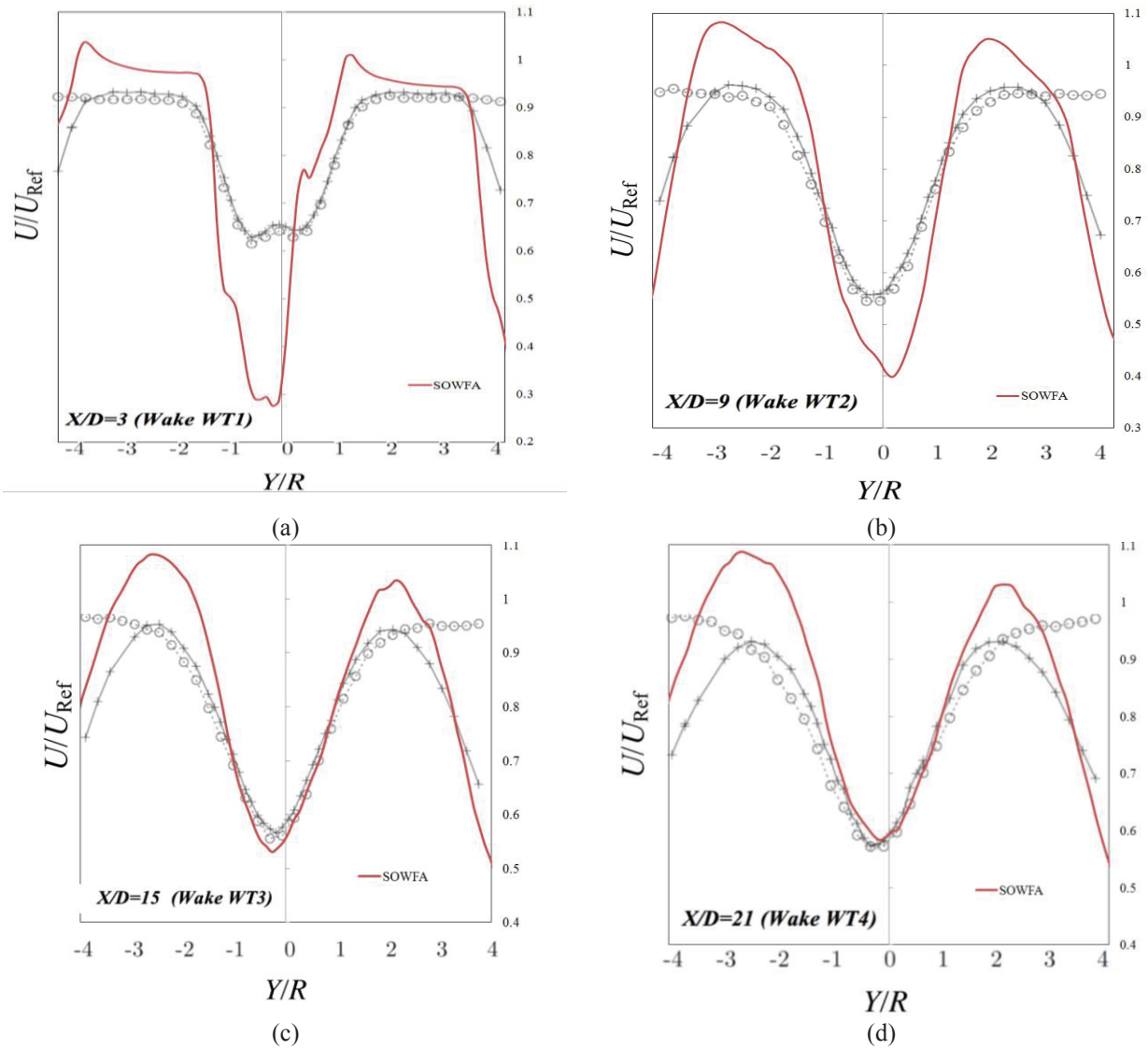

FIGURE 10. The horizontal velocity profiles behind the wind turbines of the central row in sections X / D = 3 (a); 9 (b); 15 (c); 21 (d), where X is the distance from the first wind farm, D is the diameter of the turbines

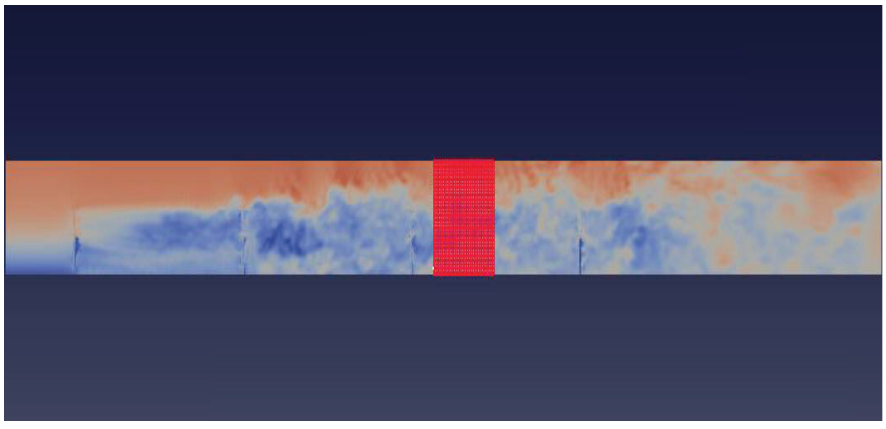

FIGURE 11. 3D box in numerical domain for calculation E(k)

In order to study the value of Energy Spectrum E(k) with FFTW library a 3D box comprising an even mesh was created (Fig. 11). The velocity field was then interpolated into the box and FFTW was applied. The calculated Energy Spectrum E(k) in Fourier space was closed to Kolmogorov-Obukhov k-5/3 spectrum (Fig. 12).

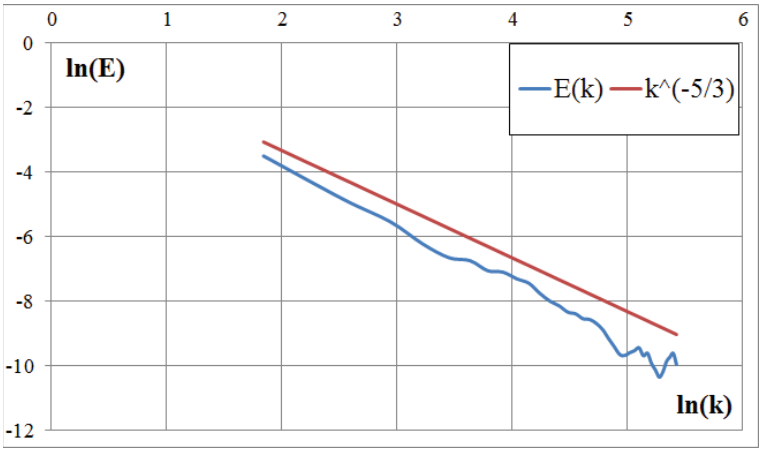

FIGURE 12. Energy spectrum E(k)

CONCLUSION

The goal of the simulations has been the measured velocity in wind turbine experiment. A turbulent wake behind model with wind turbines was studied. A LES simulation using SOWFA library was carried out with two different solvers. In connection with the small size of the wind turbines and the large speed of blades rotation we can neglect some terms like the horizontal gradient of pressure and Coriolis force in momentum equation. Thus, the pisoFoamTurbine solver can be used for simulation of turbulent flows in such cases.

The results of velocity field prediction were improved by introducing the tower and the hub geometry to the model. The final maximum discrepancy for Blind Test 4 for the normalized velocity amounts to 8% that indicates a good accuracy for engineering calculations. The difference with experiment's values of velocity profiles with 12 wind turbines in different sections can be explained by using ALM model to simulate flow around blades.

The calculations were carried out at the HPC cluster of ISP RAS with 24-96 cores per numerical case.

ACKNOWLEDGMENTS

The project was supported by RFBR (grant No. 17-07-01391).

REFERENCES

1. R.J.A.M. Stevens, C. Meneveau, Annu. Rev. Fluid Mech. **49**, 311–39 (2017).
2. D. Mehta, *et al*. J. Wind Eng. Ind. Aerodyn. **133**, 1–17 (2014).
3. M. J. Churchfield, S. Lee, J. Michalakes, and P. J. Moriarty, Journal of Turbulence **13(14)**, 1–32 (2012).
4. H. G. Weller, G. Tabor, H. Jasak, and C. Fureby, Computers in Physics **12(6)**, 620-631 (1998).
5. P. Sagaut. *Large eddy simulation for incompressible flows: an introduction* (Springer, Berlin, 2002), 426 p.
6. C. Meneveau, T. S. Lund, and W. H. Cabot, J. Fluid. Mech. **319**, 353–385 (1996).
7. F. Pierella, P. Å. Krogstad, and L. Sætran, Renew. Energ. **70**, 62–77 (2014).
8. J. Bartl and L. Sætran, Wind Energ. Sci. **2**, 55–76 (2017).
9. P. E. Hancock and F. Pascheke, Boundary-Layer Meteorol. **151**, 23–37 (2014).
10. P. E. Hancock and T. D. Farr, J. Phys.: Conf. Ser. **524**, 012166 (2014).
11. J. N. Sørensen and W. Z. Shen, Journal of Fluids Engineering **124**, 393-399 (2002).
12. A. Kryuchkova, J. Tellez-Alvarez, S. Strijhak, and J.M. Redondo, "Assessment of turbulent wake behind two wind turbines using multi-fractal analysis," in *Ivannikov ISPRAS Open Conference (ISPRAS),* (2017), pp. 110–116.